WILEY | Hindawi

Research Article

Alkaline-Stable, In Situ Menshutkin Coat and Curable Ammonium Network: Ion-Solvating Membranes for Anion Exchange Membrane Water Electrolyzers

Jiyoon Jung,[1,2,3] **Young Sang Park,**[1,2,3] **Gwan Hyun Choi,**[1] **Hyun Jin Park** ⓘ**,**[4]
Cheol-Hee Ahn,[3] **Seung Sang Hwang,**[1,2] **and Albert S. Lee** ⓘ[1,2]

[1]*Materials Architecturing Research Center, Korea Institute of Science and Technology, Hwarangno 14 gil-5, Seongbuk-gu, Seoul, Republic of Korea 02792*
[2]*Convergence Research Center for Solutions to Electromagnetic Interference in Future-mobility, Korea Institute of Science and Technology, Hwarang-ro 14-gil 5, Seongbuk-gu, Seoul, Republic of Korea 02792*
[3]*Research Institute of Advanced Materials (RIAM), Department of Materials Science and Engineering, Seoul National University, Gwanak-ro 1, Gwanak-gu, Seoul, Republic of Korea 08826*
[4]*FC Material R&D Group, KOLON Industries Inc., 110, Magokdong-ro, Gangseo-gu, Seoul, Republic of Korea 07793*

Correspondence should be addressed to Hyun Jin Park; hyunjineeee@gmail.com and Albert S. Lee; aslee@kist.re.kr

Anion exchange membranes fabricated through a one-step Menshutkin reaction with down-selected multifunctional alkyl halides and multifunctional tertiary amines within an ion-solvating matrix, poly(ethylene-co-vinyl alcohol), yielded alkaline-stable ammonium network polymers. Due to the vast simplicity in fabrication due to the quaternization/Menshutkin reaction between tertiary amine and alkyl bromides, which does not evolve any by-products that require purification, alkaline-stable membranes were fabricated in one step through facile mixing and curing of alkaline-stable ammonium network forming monomers. Prepared membranes showed controllable ion exchange capacity (IEC), conductivity, and mechanical strength by controlling of poly(ethylene-co-vinyl alcohol) amount which is an ion-solvating polymer. The selection of ammonium network chemical structure allowed for flawless retention of IEC and conductivity under conditions of 70°C, 1M KOH of over 300 h. Anion exchange membrane electrolysis membrane electrode assembly tests with optimized membranes showed a greater performance ($1.78 \, \text{A/cm}^2$ at 2.0 V) and more enhanced water electrolyzer durability than that of commercial anion exchange membrane.

1. Introduction

Water electrolysis is a technology that produces hydrogen and oxygen through the electrochemical splitting of water molecules. Water electrolysis can be categorized into alkaline water electrolysis (AWE), proton exchange membrane water electrolysis (PEMWE), anion exchange membrane water electrolysis (AEMWE), and solid oxide water electrolysis (SOWE). AWE using high concentration of KOH supporting electrolyte is known so far as to be the most economical, but low hydrogen production rates and gas crossover caused by using a porous separator severely hinder its application [1, 2]. PEMWE uses a cation exchange membrane, and protons move through the membrane with pure water as electrolyte. While PEMWEs are able to achieve higher current densities compared with AWEs, which is directly related to hydrogen production rates, high costs associated with balance-of-plant components and use of expensive platinum group metals as catalysts are difficult challenges to overcome [3, 4]. AEMWE combines the advantages of AWE and PEMWE through the potential integration of non-PGM catalysts and solid-state anion exchange membrane (AEM),

which mitigates gas crossover. However, since AEMWE operates under alkaline condition, the alkaline stability of AEM is a critical component of cell durability [5–9].

The anion exchange membrane (AEM) serves two main roles. First, it must selectively transfer hydroxide ions through the cation head group as to impart high ionic conductivity. Second, it must act as a physical barrier to prevent the crossover of hydrogen and oxygen [10]. Moreover, as the nature of charged membranes, the physical properties such as water uptake (WU), ion exchange capacity (IEC), and their effect on mechanical properties are almost always in a tradeoff relationship [11, 12]. Also, as these membranes are utilized under alkaline conditions, hydroxide ions attack the backbone and cation groups of the polymer, reducing the long-term durability of AEMWE [13–17]. Thus, it is important to develop AEMs with high durability under alkaline environment to ensure the performance and durability of the cell.

In AEMs, quaternary alkyl ammonium (QA) groups and imidazolium (IM) groups have mostly been studied as ion exchange functional groups [9, 18, 19]. Although QA and IM groups show good ionic conductivity, they are susceptible to degradation under alkaline conditions through SN2 reaction, Hofmann elimination, and C2 substitutions. Among ammoniums, Marino and Kreuer found that alkaline stabilization of N,N-dimethyl piperidinium (DMP) and 6-azaspiro(5,5)undecanium (ASU) groups was excellent [20]. Under conditions of 160°C in 6 M NaOH, the half-life of trimethylamine (TMA) group is 61.9 h, but DMP and ASU groups have excellent half-life of 87.3 h and 110 h, respectively. In the DMP and ASU groups, all β hydrogens are inside the ring, so SN2 and E2 reactions do not occur readily due to steric hindrance. Furthermore, the backbone structure of AEMs is also crucial. The polymer backbone carries cationic groups and preserves the dimensional stability of the membranes [21]. Most AEMs consist of a rigid aromatic polymer backbone, which provides good mechanical strength and film-forming abilities, but their low water uptake and brittleness negatively affect the operation of cells [22]. In addition, poly(2,6-dimethyl-1,4-phenylene oxide)-(PPO-) based AEMs have been widely studied as AEM materials due to their relatively easy synthesis method and excellent thermal and mechanical stability [23–26]. However, the aryl-ether bond is easily attacked by hydroxide and degradation occurs, so vulnerable to alkaline condition. In order to increase the alkaline stability of the backbone, there are many studies on aryl-ether free polymer [27–30]. In recent study, poly(fluorenyl-co-aryl piperidinium)-based AEMWEs using PGM catalysts showed an outstanding current density of 7.68 A cm^{-2} at a cell voltage of 2.0 V and a durability of 1,000 hours due to the aryl-ether free backbone and cyclic QA groups [31].

A blend membrane is one prepared by simply mixing two or more different polymers, and an interpenetrating polymer network (IPN) is a membrane in which different polymers coexist and form a separate network. Ion-solvating materials have a polymeric backbone with affinity for aqueous KOH to which the membrane is absorbed, so often used as a blending material to increase mechanical strength while increasing ionic conductivity [32]. Especially,

poly(vinyl alcohol) (PVA) is a hydrophilic polymer containing a lot of hydroxide groups, which enable conductivity improvement, and as such has been investigated as ion-solvating matrix in various AEM studies. Yang et al. fabricated a semi-IPN membrane of 1-vinylimidazole functionalized BPPO (VImPPO) and PVA using the thiolene reaction [33]. The flexible PVA and rigid PPO-based polymer showed high mechanical strength up to 30.8 MPa while showing IEC of 1.46 meq g^{-1}. Wang et al. synthesized quaternized PVA (QPVA) to increase the conductivity of AEM and fabricated semi-IPN with QPVA and poly(diallyldimethylammonium chloride). Thereafter, cross-linking was performed using glutaraldehyde to enhance the dimensional stability of QPVA, and the QPVA/PDDA0.5-GA membrane exhibited an ionic conductivity of 21.8 mS cm^{-1} at room temperature. Also, Park et al. prepared a blending membrane for AEMWE using poly(1-vinyl-3-imidazole-co-styrene) (PIS) and PVA [2]. The PISPVA46 membrane showed a high water uptake of 101.1% and ionic conductivity of 89.7 mS cm^{-1} at 0.5 M KOH and 60°C. In addition, it showed current density of 457.7 mA cm^{-2} at cell voltage of 2.0 V in 0.5 M KOH environment. However, even when cross-linked, PVA still shows high water uptake ability and low-dimensional stability due to tremendous -OH groups. In addition, water solubility changes depending on the degree of saponification and molecular weight of PVA, and it is difficult to be applied in temperatures above 50°C as it becomes soluble in water. By contrast, ethylene vinyl alcohol (EVOH) is a thermoplastic copolymer of vinyl alcohol and ethylene. With a higher Tg than that of PVA, insolubility in water under any temperature condition, and high mechanical properties, EVOH is an attractive commercial polymer matrix to supplant PVA as an ion-solvating matrix.

In general, in order to synthesize AEMs, several complex synthesis processes, precautions, or catalysts are required, which is an obstacle to commercialization. For example, in the case of free radical polymerization using a vinyl-based monomer, oxygen removal is very important because oxygen binds to radicals and interferes with polymerization [34]. In some cases, expensive Grubbs polymerization catalyst or corrosive superacids are used to synthesize AEMs [35–39].

In this study, using the Menshutkin reaction of commercially available low-cost monomers, we developed a method for manufacturing AEMs in a vastly simplified method through one-step fabrication without using any catalyst. After mixing trifunctional alkyl bromide with benzene ring, monomer containing two methyl piperidines, and EVOH solution, the casting solution was placed in an oven at 80°C. Excess solvent is slowly evaporated while the Menshutkin reaction between the bromomethyl groups and piperidine groups is completed. After that, the membrane was finally fabricated through cross-linking of EVOH using GA. The prepared AEMs are expected to exhibit good alkaline stability as all of the beta hydrogens are within the piperidinium ring.

2. Materials and Methods

2.1. Materials. 1,3,5-Tris(bromomethyl)benzene (97%), 4,4′-trimethylenebis(1-methylpiperidine) (98%), poly(vinyl

alcohol-co-ethylene) (ethylene group 32 mol %, EVOH), and poly(vinyl alcohol) (PVA) with Mw of 89,000-93000 were received by Sigma-Aldrich Chemical Co. Ltd. and used as received. n-Propyl alcohol (NPA), dimethyl sulfoxide (DMSO, 99.5%), ethyl alcohol (99.5%), hydrochloric acid (35~37% aqueous solution, HCl), potassium hydroxide (KOH), and glutaraldehyde (GA, 25 wt% aqueous solution) were obtained from Daejung and used as received.

For AEMWE cell test, platinum ruthenium (50 wt% Pt-50, 25 wt% Ru-25, 047371.06) on the cobalt nanopowder (99.8%, 46347), iridium(IV) oxide (99.99 wt%, 043396.06), and carbon support were supplied by Alfa Aesar. FAA-3-50 membrane was received from FumaTech.

2.2. PiP/xEVOH Interpenetrating Network Membrane Preparation.

A network containing piperidinium cations was expressed as PiP, and the weight percent (wt %) of the EVOH in the membrane is represented by x. For the fabrication of the PiP/xEVOH membranes, a total of three solutions of two monomer solutions and an EVOH solution were prepared. 1,3,5-Tris(bromomethyl)benzene (1.0 g, 2.80 mmol) and 4,4′-trimethylenebis(1-methylpiperidine) (1.0 g, 4.20 mmol) were dissolved in 9 g of DMSO, respectively. In another vial, 20 g of EVOH solution in DMSO (10 wt%) was prepared. After mixing the three solutions at once, well-mixed solution was casted on a glass plate. The solvent was evaporated while cross-linking through Menshutkin reaction that took place within the EVOH matrix for 24 h in a convection oven at 80°C. After that, the cast membranes were in 100°C vacuum oven over 48 h to evaporate off remaining DMSO solvent. Then, the cross-linked membrane was removed from the glass plate and PiP/50EVOH was obtained. In the same way, PiP/60, 70, and 80 EVOH were obtained by adjusting the ratio of the PiP cation network and EVOH.

The hydroxyl group in the EVOH was cross-linked using GA to enhance the dimensional stability of the anion exchange membrane. By diluting the 25% GA aqueous solution with ethyl alcohol, 5% GA solution was prepared and pH was adjusted to 3 with HCl. Synthesized IPN membrane was immersed at 70°C for 24 h. Finally, PiP/xEVOH was gained through washing and drying.

2.3. Characterization and Measurements.

Fourier-transform infrared spectroscopy (FT-IR) spectra were obtained using PerkinElmer FT-IR system (Spectrum-GX) produced by ATR to analyze the structure of AEMs. The thermal property of the PiP/xEVOH was examined by TA Instrument TGA 2950 with 10°C/min heating rate under N_2 atmosphere. Mechanical property of the membranes was characterized using universal tensile machine (Tinius Olsen H5K-T). Membrane samples (4 cm ∗ 0.5 cm) were prepared to measure the mechanical strength and investigated at 10 mm/min stretching speed.

Ion exchange capacity (IEC) value was confirmed by the back titration. Membranes with hydroxide counter ions were immersed in HCl solution (0.01 M) for 24 h. The HCl solution was back titrated using KOH aqueous solution (0.01 M) after adding three or four drops of 1% phenolphthalein solution in ethanol. The IEC (meq g^{-1}) was obtained based on the following formula:

$$\text{IEC} = \frac{V\text{HCl} \times C\text{HCl} - V\text{NaOH} \times C\text{NaOH}}{W\text{dry}}, \quad (1)$$

where V_{HCl} and V_{NaOH} are the volumes of HCl and NaOH, respectively. C_{HCl} and C_{NaOH} are the concentrations of HCl and NaOH, respectively. W_{dry} is the weight of the dried membranes.

The water uptake (WU) and swelling ratio (SR) were evaluated after immersing the membrane in water at RT for 24 h. After taking out the membrane, surplus water on the surface was carefully wiped off and the weight and length were measured for comparison. After the membrane was completely dried, the length and the weight of the dried membrane were also measured. As the result, SR and WU were calculated according to the following formula:

$$\text{SR} = \frac{L\text{wet} - L\text{dry}}{L\text{dry}} \times 100\%,$$
$$\text{WU} = \frac{W\text{wet} - W\text{dry}}{W\text{dry}} \times 100\%. \quad (2)$$

The KOH uptake was tested in the similar method. The prepared membrane was soaked in 1 M KOH at 25°C for 24 h. The weight of the membrane was measured after eliminating the surplus KOH solution on the surface of the membrane. After washing two or three times with distilled water and drying, the membrane's weight was measured. KOH uptake was finally obtained using the following formula:

$$\text{KOH uptake} = \frac{m\text{wet, KOH} - m\text{dry}}{m\text{dry}} \times 100\%. \quad (3)$$

The ohmic resistance of the AEMs was measured in water and 0.1 M-5 M KOH solutions at different temperatures by two-electrode AC impedance spectroscopy on a Solartron 1260 in the 10 Hz to 10 MHz frequency range with an amplitude of 20 mV. To equilibrate in water, all the membranes with OH$^-$ counter ions were soaked in distilled water over 24 h. Hydroxide conductivity was determined from the following formula:

$$\sigma = \frac{L}{W \times R \times d}, \quad (4)$$

where L and R were the distance between two electrodes (cm) and the obtained ohmic resistance (Ω), respectively. W and d were the width (cm) and thickness (cm) of the membrane, respectively.

2.4. Membrane Electrode Assembly (MEA) Preparation and AEMWE Performance.

MEAs (1 or 5 cm^2 active area) with PiP/xEVOH were prepared by the catalyst-coated substrate (CCS) method. PtRu/C (50 wt%) was used as cathode for preventing phenyl adsorption effect containing TMA-70

ionomer [40], and IrO$_2$ and Co were used as anode catalysts. To prepare the catalyst inks, each catalyst powder was dispersed with TMA-70 ionomer which was synthesized following the literature procedure [41] (Figure S1) (TMA-70 4.65 wt% solution in water: n-propanol 1:1 wt, the I to C weight ratio is 0.5, and for the OER catalyst layer, the binder content was 10 wt%) in water and n-propanol mixture, and ultrasonic treatment was successively done over 20 min keeping water temperature under 35°C to inhibit catalyst agglomeration. Catalyst ink was instantly sprayed on the gas diffusion layer (GDL) set on a 70°C heating plate. For the anode and cathode GDLs, Pt-coated Ti paper (Giner) and 39 BB (Fuel Cell Store) were used, respectively. Cathode catalyst loading amount is 0.6 mgPt cm^{-2}, and anode catalyst loading content is 2.0 mgIr cm^{-2}, 0.7 mgCo cm^{-2}. The prepared CCS was dried at RT over an hour to get rid of surplus solvent. Before the single cell test, the PiP/xEVOH membranes were placed in the middle of the fabricated electrode. Polarization curves were gained with water electrolysis MEA single cell (Scribner) powered by a BioLogic potentiostat (SP-200) connected to a power booster (HCV-3048), while the electrolyte was delivered using a peristaltic pump.

3. Results and Discussion

3.1. Preparation and Characterization of PiP/xEVOH Interpenetrating Network Membrane. PVA is a hydrophilic polymer, as it contains abundant hydroxyl groups and has good film-forming property. However, high water uptake due to the abundant hydroxyl groups of PVA greatly affects the dimensional stability of AEMs [42, 43]. Also, PVA dissolves in water at mildly elevated temperature, limiting the operation temperature to below 60°C of any electrochemical cell containing it. As such, an alternative ion-solvating polymer, poly(vinyl alcohol-co-ethylene) (EVOH) with fewer hydroxyl groups, was used instead of PVA to improve the dimensional stability and mechanical stability. EVOH has lower flexibility and water uptake than those of PVA [44], but still has good film-forming property and is insoluble in water. In addition, EVOH contains ethylene group in the backbone structure enhancing its mechanical strength made it higher than that of PVA [45].

In order to justify our use of EVOH over PVA, we initially tested its mechanical properties as shown in Figure S2. As shown, the mechanical properties of the cross-linked PVA and EVOH freestanding films under dry and wet conditions revealed that the PVA film showed high elongation at break of 278% under dry conditions and tensile strength of 39.8 MPa. However, in the same condition, EVOH showed a relatively low elongation at break of 9.1%, but showed a higher mechanical strength of 47.8 MPa. EVOH films were poor in ductility compared to PVA films due to the ethylene groups in the backbone, and these properties were obtained with low strains of EVOH. Since EVOH will form IPN with the cation network, the low elongation at break value of EVOH compensates the high elongation at break value of the cation network, so consequently, it is expected to increase the dimensional

stability of the IPN membrane. After immersing the freestanding film in water for more than 24 h, the elongation at break of PVA increased to 583%, but the tensile strength was decreased by 12.9 MPa, while the wet EVOH film showed a slight increase in elongation at break and excellent tensile strength of 32.2 MPa. Thus, the higher mechanical strength under both dry and wet conditions as well the relatively lower drop-off in tensile strength when wet was the main reasoning and rationale behind the selection of EVOH over PVA as IPN counterpart.

For the cationic network, we took a closer look at the nature of the Menshutkin reaction, which is a reaction between tertiary amines and alkyl halides to quantitatively form quaternary amines or ammonium groups, without the formation of any by-products. Understanding these parameters, we selected tris(bromomethyl)benzene, a trifunctional alkyl halide, and 4,4′-trimethylenebis(1-methylpiperidine), difunctional piperidine, which under 1:1 stoichiometric input of alkyl halide:piperidine ratio, may form a highly cross-linked quaternary ammonium network polymer. As such, to fabricate the IPN membrane, a solution of EVOH and alkyl halide monomer and another with the aforementioned piperidine were prepared and the two solutions were mixed, and the mixture solution was poured into a mold and the solvent was slowly evaporated while cross-linking at 80°C. In order to insure the premature Menshutkin cross-linking of the monomers, the casting solution was held at total solid content of 5 wt%. Also, DMSO was used as the solvent as it can dissolve both monomers and EVOH, and the complete Menshutkin reaction was observed in the DMSO/EVOH matrix. It is noteworthy to point out due to the high boiling point of DMSO that the time it takes to fully evaporate this casting solvent provides sufficient mixing time for homogeneous solubilization of the monomers within the EVOH matrix, and eventually, full conversion of both alkyl halide and piperidine groups to form piperidinium cationic networks took place in the solid state after DMSO was fully evaporated.

This synthesis scheme is detailed in Figure 1(a). Through the Menshutkin reaction of the bromomethyl group of 1,3,5-tris(bromomethyl)benzene and the piperidine group of 4,4′-trimethylenebis(1-methylpiperidien), a cross-linked structure was formed and ion exchange groups were created at the same time. Finally, to fabricate the PiP/xEVOH IPN membrane, semi-IPN with the cation network and the EVOH was cross-linked with the EVOH hydroxide group using GA via formation of acetal bonds. Cross-linking reaction mechanism between EVOH and GA is shown in Figure S3. A network containing piperidinium cations was expressed as PiP. The weight percent (wt %) of the EVOH in the membrane is represented by x and the PiP content in the membrane as (100-x) %. The PiP/xEVOH membrane was prepared with different EVOH contents in the range of 50-80 wt%. When the EVOH content was less than 50 wt%, the IEC was too high, making it difficult to handle under wet conditions. Figure 1(b) shows the yellowish transparent PiP/xEVOH membrane, and Figure S4 shows SEM images and EDX images of the cross section of the PiP/xEVOH membrane. In the EDX images, the element O present in EVOH and the
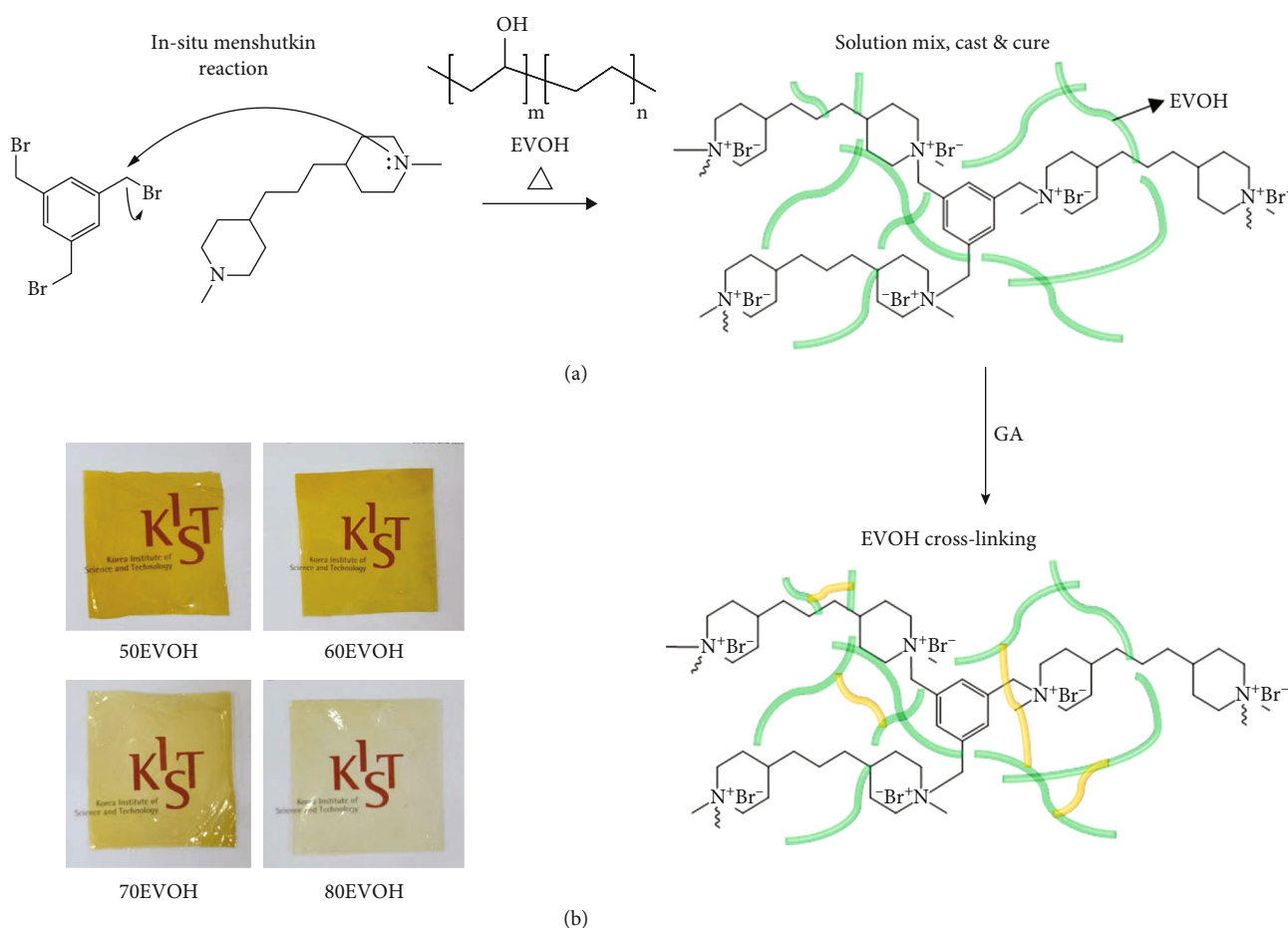
(a)

(b)

FIGURE 1: (a) Fabrication process of PiP/xEVOH AEMs. (b) Image of PiP/xEVOH AEMs according to EVOH content.
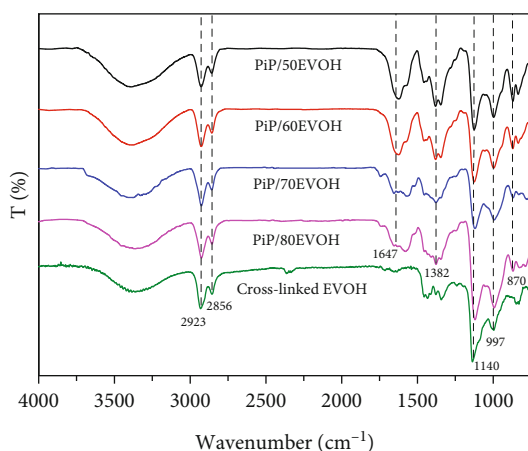

FIGURE 2: FT-IR spectra of the PiP/xEVOH membranes with diverse EVOH content.

element Br present in PiP were evenly mixed without phase separation. Therefore, the PiP/xEVOH membrane was shown to be of homogenous and dense structure.

Figure 2 shows FT-IR spectra of cross-linked EVOH film and the PiP/xEVOH membrane with EVOH content of 50-80 wt%. -OH peak was observed at ~3000 cm^{-1} due to the

hydroxyl group of EVOH in all membranes. EVOH peaks were observed at 2923 cm^{-1} (CH$_2$ antisymmetric stretching), 2856 cm^{-1} (CH$_2$ symmetric stretching), 1140 cm^{-1} (C-O), 1150-1085 cm^{-1} (C-O-C), and 997 cm^{-1} (acetal group) [46, 47]. In the PiP/xEVOH membrane, peak of 1647 cm^{-1} indicating the stretching vibration of quaternary ammonium groups increased as the PiP content increased. Also, the PiP/xEVOH membrane-related peaks are observed at 1382 cm^{-1} (C-N) and 870 cm^{-1} (aromatic C=C and C-H stretch).

As the operating temperature of AEMWE is 60-80°C, the AEMs should have high thermal stability. The thermal stability of cross-linked EVOH and the PiP/xEVOH membrane was analyzed by TGA as depicted in Figure S5. EVOH showed high thermal stability up to 300°C, and thermal degradation of EVOH backbones started at 310°C. Moreover, all the PiP/xEVOH AEMs were stable up to 200°C and exhibited excellent thermal stability. In PiP/xEVOH, the decomposition of piperidinium cations started around 200°C, which is a characteristic of ammonium-functionalized polymers.

Figure 3 shows the mechanical properties of the PiP/xEVOH membranes. The PiP/xEVOH membranes showed high mechanical strength that ranged from 21.9 to 55.3 MPa, which is indicative of excellent mechanical strength imparted by the cross-linked EVOH and
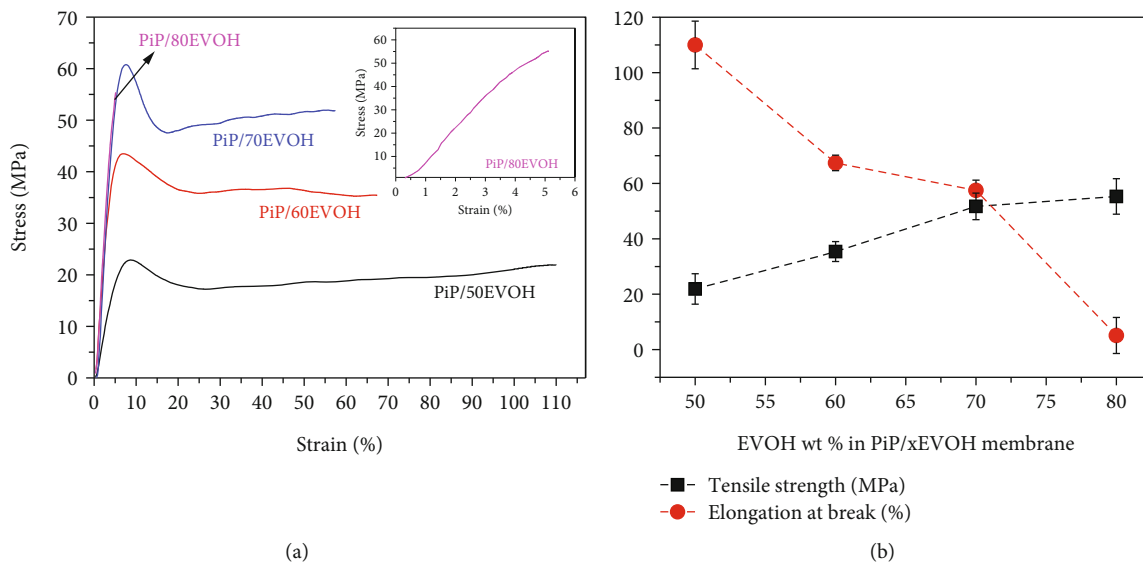
(a)

(b)

FIGURE 3: (a) Stress-strain curves of PiP/xEVOH. (b) Summary of mechanical properties of PiP/xEVOH.

TABLE 1: Physical properties of PiP AEMs.

Sample	IEC (meq g^{-1})		Water uptake (%)[c]	Swelling ratio (%)[d]	KOH uptake (%)[e]	Ionic conductivity (mS cm^{-1})[f]	
	Theoretical[a]	Measured[b]				25°C	70°C
FAA-3	—	2.01	41.6	13.5	80.2	23.4	59.6
Cross-linked PVA	—		19.3	10.7	19.3	—	—
Cross-linked EVOH	—		8.4	4.2	7.3	—	—
PiP/50EVOH	1.98	1.46	37.9	11.2	60.9	41.4	66.6
PiP/60EVOH	1.57	1.38	35.5	10.9	53.1	35.2	54.4
PiP/70EVOH	0.98	0.88	20.3	4.6	28.8	26.8	51.6
PiP/80EVOH	0.82	0.70	17.2	4.4	14.7	21.2	49.3

[a]Calculated theoretical IEC after removal of unreacted monomer. [b]Measured by acid-base titration. [c,d,e]Measured at 25°C. [f]Measured at 100% RH.

interpenetrating cationic network. PiP/80EVOH showed excellent mechanical property of 55.3 MPa but showed low elongation at break of 5.1% due to the low elongation at break of EVOH freestanding film as shown in Figure S2. As the EVOH content increased, tensile strength increased while elongation at break decreased as expected. Moreover, Figure S6 compares the mechanical properties between PiP/60PVA and PiP/60EVOH, and we were able to observe a higher tensile modulus of 35.4 MPa greater than that of PiP/60PVA.

3.2. Hydration Properties of PiP/xEVOH Anion Exchange Membranes.

The IEC, water uptake, swelling ratio, KOH uptake, and ionic conductivity values of the PiP/xEVOH membranes are summarized in Table 1. As IEC value indicates the equivalent of ion exchange groups per weight (g) of the membrane, a higher IEC leads to the better ionic conductivity [48, 49]. As can be seen in Table 1, the PiP/xEVOH membrane shows higher IEC values with the content of PiP increases, and the highest IEC value of PiP/50EVOH exhibited 1.46 meq g^{-1}.

The cross-linked EVOH freestanding film showed alkaline 1 M KOH solution uptake value of 7.3% which is smaller than that of cross-linked PVA. As such, as the EVOH content decreases, water uptake, swelling ratio, and KOH uptake increase, which shows good accordance with the IEC results and related graph is shown in Figure S7. PiP/50EVOH exhibited the highest uptake with 37.9% water uptake and 60.9% KOH uptake. PiP/50EVOH showed a high level of KOH uptake because of the influence of the cationic network.

3.3. Ionic Conductivity.

The ionic conductivity of the PiP/xEVOH membrane is shown in Figure 4(a). As expected, the PiP/50EVOH membrane with the highest IEC showed the highest ionic conductivity of 66.6 mS cm^{-1} at 70°C. As the cationic network content decreased, the ionic conductivity decreased. Figure 4(b) describes the hydroxide conductivity of the PiP/50EVOH and FAA-3-50 membranes at different temperatures. FumaTech's FAA-3 is a commercially available AEM that consists of a polyaromatic backbone and quaternary ammonium side chain. The IEC value
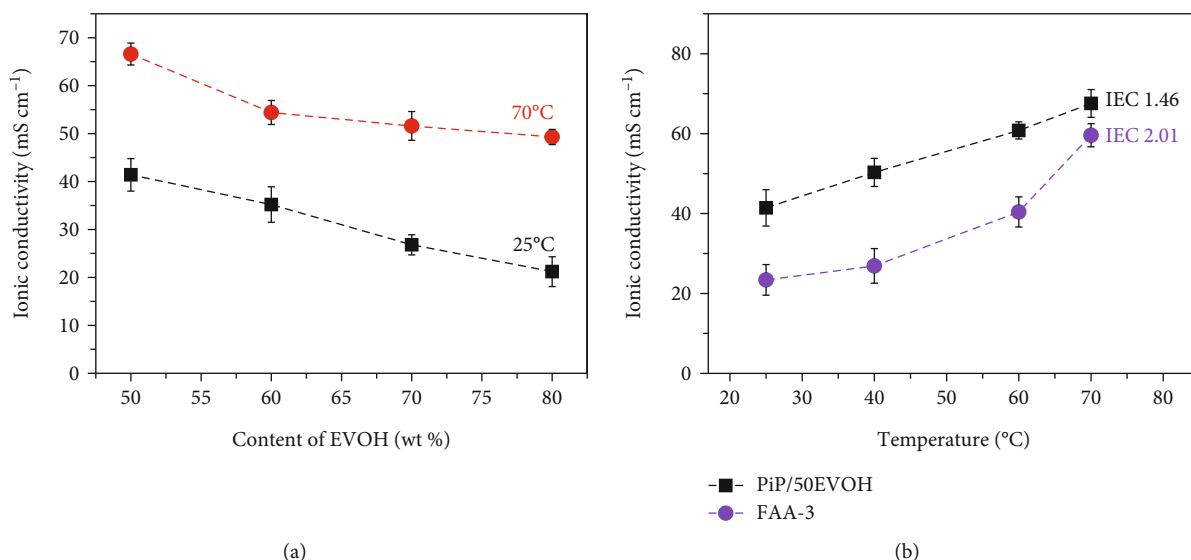
(a)

(b)

FIGURE 4: (a) Hydroxide conductivity of the PiP/xEVOH AEMs. (b) Hydroxide conductivity of the PiP/50EVOH membrane and FAA-3 at different temperatures.

of FAA-3 is 2.01 meq g^{-1}, which has a higher IEC value than that of PiP/50EVOH (1.46 meq g^{-1}). However, in all temperature ranges, PiP/50EVOH showed higher ionic conductivity. Since the hydroxide group of EVOH is not a cationic group, so it does not influence the IEC value, but still the hydroxide group in the EVOH also can transfer the hydroxide ion by the Grotthuss mechanism [42].

As AEMWEs operate with an alkaline solution, the hydroxide conductivity in KOH solution was confirmed. As shown in Figure S8(A), the PiP/50EVOH membrane showed high ionic conductivity as the temperature increased in 1 M KOH and 79 mS cm^{-1} of ionic conductivity obtained at 70°C. Figure S8(B) shows the ionic conductivity of the PiP/50EVOH membrane according to the KOH concentration at 70°C. As the KOH concentration increased, the ionic conductivity increased and the PiP/50EVOH membrane reached a high ionic conductivity of 225 mS cm^{-1} in 5 M KOH solution.

3.4. Alkaline Stability. The alkaline stability of AEM is an important issue because it affects the long-term durability and efficiency of AEMWE. It has been well known that the backbone structure of the polymer and the surrounding structure of the quaternary ammonium group have a great influence on alkaline stability [27, 28]. The aryl-ether bond, which is easily degraded by the attack of hydroxide ions, and the quaternary ammonium groups are also attacked by hydroxide ions through Hofmann elimination or SN2 reaction. The quaternary ammonium groups in which β hydrogens exist inside the ring are not readily accessed by hydroxide ions through steric hindrance, so piperidinium and pyrrolidinium cations have been touted as good candidates for cation groups [20].

To confirm the alkaline stability of PiP/50EVOH and FAA-3, IEC and ionic conductivity retention tests were performed according to immersion time in 1 M KOH at 70°C, as shown in Figure 5. Both IEC and ionic conductivity of

FAA-3 decreased over time. In particular, the ionic conductivity dropped sharply to a mere 12% of the initial value after 300 h of immersion. By contrast, the IEC and ionic conductivity of PiP/50EVOH only slightly decreased compared to the initial values, and the IEC showed higher values after immersion in 1 M KOH at 70°C for 300 h and had an excellent ionic conductivity retention than those of FAA-3. This could be attributed to the stability of the cyclic quaternary ammonium groups of piperidinium.

Figure S9 shows the mechanical strength change of PiP/60EVOH before and after immersing in 1 M KOH at 70°C for 300 h. Although the tensile strength decreased from 35.4 MPa to 31.0 MPa, it still maintained high mechanical strength at 87.6% of the initial level. Figure S10(A) shows the FT-IR changes of PiP/50EVOH before and after immersing in 1 M KOH at 70°C for 300 h. After 300 h, the quaternary ammonium peak decreased slightly, and the C-N peak at 1382 cm^{-1} was broadened, confirming that degradation of quaternary ammonium occurred. In addition, 997 cm^{-1} peak increased due the generation of secondary and primary alcohol, and 1127 cm^{-1} peak was decreased which means the C-O-C in EVOH was destroyed. Degradation of the acetal group of EVOH is the major degradation mechanism because there is no significant decrease in ionic conductivity or IEC. Based on this, the major and minor degradation mechanisms are shown in Figure S10(B).

3.5. Anion Exchange Membrane Electrolysis Cell Performance. The fabricated PiP/xEVOH membranes were then subjected to membrane electrode assembly tests to demonstrate their applicability to AEMWEs. All four developed PiP/xEVOH AEMs ($x = 50, 60, 70, 80$) were tested, and their cell performance was compared under conditions of 1.0 M KOH circulating electrolyte at 70°C as shown in Figure 6. Initial performance of polarization curves showed that the lowest content of EVOH with PiP/xEVOH series exhibited the best cell performance, among four different contents, with
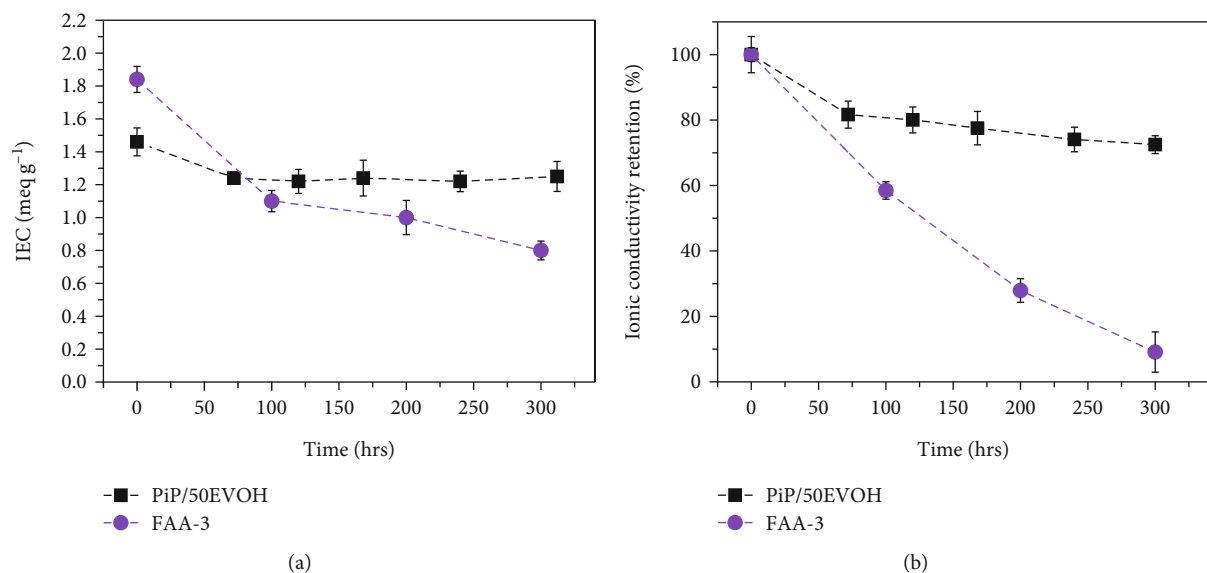
(a)

(b)

FIGURE 5: Alkaline stability of PiP/50EVOH and FAA-3 in 1 M KOH at 70°C for 300 h: (a) ion exchange capacity and (b) ionic conductivity retention.
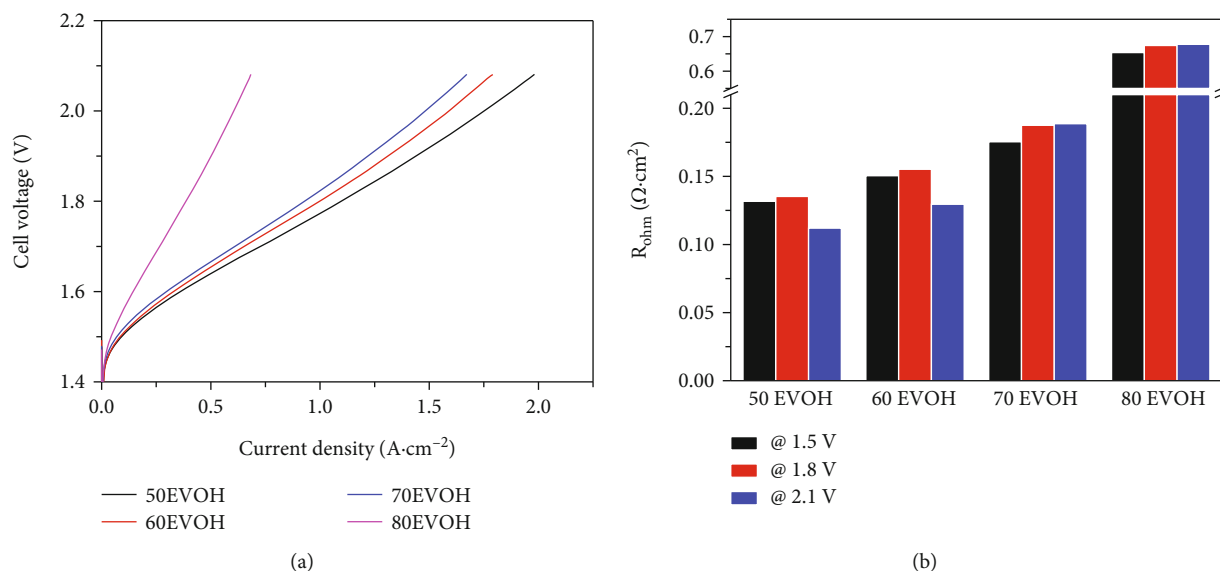

(a)

(b)

FIGURE 6: Electrochemical analysis of AEMWE with diverse EVOH content: (a) polarization curves and (b) EIS Nyquist plot.

maximum current density of $1.78\,A\,cm^{-2}$ at 2.0 V. In addition, the current densities of other EVOH contents were $1.61\,A\,cm^{-2}$ ($x = 60$), $1.50\,A\,cm^{-2}$ ($x = 70$), and $0.61\,A\,cm^{-2}$ ($x = 80$) at 2.0 V, respectively. The single cell performance results were consistent with the trend of ionic conductivity at 70°C and hence reflected in the ohmic resistance trend in electrochemical impedance spectroscopy (EIS) analysis (Figure 6(b)) at 1.5 V, 1.8 V, and especially at 2.1 V [50, 51]. Current density performance with the PiP/80EVOH membrane is noticeably decreased, and this was attributed to the effect of percolation of hydrated clusters which enable broad range ionic conduction when it reaches threshold [52–54]. By contrast, the membranes with 50-70 EVOH have enough cat-

ionic groups so have sufficient hydrated clusters under water uptake statement; therefore, ionic conduction occurs continuously. But for PiP/80EVOH, it may be under this ammonium polymer network percolation threshold resulting in a rapid drop in AEMWE performance. This trend does not appear in the ionic conductivity that can be measured simply by putting cell in water, but shown at the AEMWE cell performance measured in voltage-applied and multifactorial environments.

Furthermore, MEA performance showed a high dependence on electrolyte concentration as shown in Figure S11(A). Even though the ionic conductivity trend increased with the concentration of KOH doping and submersion condition,

this trend was only reflected in cell performance until the electrolyte concentration was 1.0 M. After the concentration increases more than 2.0 M, the polarization curves showed decreased performance. This was attributed to previous reports in which an increase in KOH concentration results in decrease in the ohmic resistance of the membrane and increase in the reaction kinetics of OER and HER, resulting in improved AEMWE performance [55]. However, this effect is limited in a high-concentration KOH solution. At high KOH concentrations, water structure on electrode-electrolyte interface changes which leads to performance decay [56]. As the KOH concentration increases, tetrahedrally coordinated water which has the highest water dissociation energy increases that gave unfavorable influence on HER activity. In addition, the viscosity of the solution increases as the KOH concentration increases, and high viscosity may adversely affect OER and HER kinetics.

As shown in Figure S11(B), cobalt, which has been reported one of the best non-PGM OER catalyst [57], was also tested with a low loading content of $0.7 \, mgCo \, cm^{-2}$. The dependence on electrolyte concentration was similar to the MEAs fabricated with IrO_2 PGM OER catalyst. Under 1 M KOH conditions, the MEA fabricated with non-PGM catalyst Co exhibits an excellent current density of $1.2 \, A \, cm^{-2}$ at 2.0 V and 70°C, which was not significantly lower than that of the best PGM OER performance under identical testing conditions, $1.78 \, A \, cm^{-2}$ at 2.0 V and 70°C (Figure S11(C)).

In AEMWE performance, MEA with the commercially available FAA-3 membrane which is fully anion exchange membrane showed slightly higher performance than MEA with the PiP/50EVOH membrane (Figure S12). A complete AEM has much higher IEC and a faster rate of ion transport through abundant cationic groups, leading to good performance. On the other hand, PiP/xEVOH is a membrane that combines cationic network and EVOH to improve mechanical property and alkaline stability even with a slight loss in performance. In order to confirm the stability of the membranes, single cell durability test was performed at a constant voltage of 1.6 V at 70°C and compared the initial current density retention (Figure 7), following a literature [58]. The PiP/50EVOH was stably operated compared to the FAA-3 membrane for 14 h due to time constraints. While the PiP/50EVOH MEA maintained its initial current density very well without degradation, the FAA-3 cell exhibited gradual cell performance decrease within a few hours. It was noteworthy that the durability results trended differently from the alkaline stability test shown in Figure 5, as the applied voltage conditions of the MEA environment are much harsher. Some other considerations that may affect the durability may be related to the interface between catalyst layer and membrane. As we utilized a highly quaternized polystyrene-based ionomer which has high IEC of $3.3 \, meq \, g^{-1}$ for all MEAs, the interface between may be improved with more hydrophilic membranes. Nevertheless, our PiP/50EVOH membrane showed better durability than the commercially available FAA-3 membrane due to the alkaline-stable ring structure of quaternary ammonium group and stable conductivity
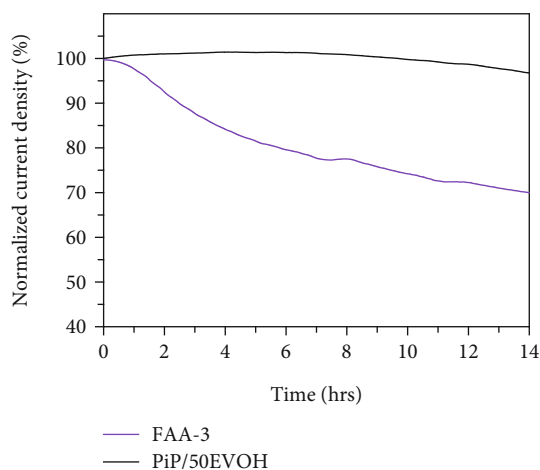

FIGURE 7: Single cell durability test of PiP/50EVOH and FAA-3 AEMWE at a constant voltage of 1.6 V at 70°C.

under corrosive alkaline electrolyte circulating conditions. Further works are ongoing to optimize MEA performance.

4. Conclusion

The EVOH-supported cationic network IPN membranes were prepared via in situ Mensutkin coat and cure method. The IEC was able to be controlled by adjusting the EVOH content, and PiP/50EVOH has an IEC of $1.46 \, meq \, g^{-1}$. The PiP/xEVOH membranes are capable of high KOH uptake of 60.9% while maintaining excellent mechanical strength of 21.9-55.3 MPa. Despite having a lower IEC value than the commercially available FAA-3 membrane, PiP/50EVOH showed a higher ionic conductivity of $66.6 \, mS \, cm^{-1}$ at 70°C due to the transport of hydroxide ions through the hydroxyl group in EVOH. Also, PiP/50EVOH which β hydrogens of cation groups exist inside the ring shows better alkaline stability than FAA-3. Under 1 M KOH conditions, MEA with the PiP/50EVOH membrane exhibits a current density of $1.78 \, A \, cm^{-2}$ at 2.0 V and 70°C. This study also showed the performance of $1.2 \, A \, cm^{-2}$ at 2.0 V with a non-PGM Co OER catalyst, which was a small drop off from the PGM IrO_2 catalyst. Consequently, considering the simple membrane fabrication and the excellent alkaline stability, our EVOH-supported cationic network IPN membranes will open up opportunities as alternative anion exchange membrane materials for various applications.

Data Availability

The data that support the findings of this study are available from the corresponding authors upon reasonable request.

Conflicts of Interest

The authors declare that they have no known competing financial interests or personal relationships that could have appeared to influence the work reported in this paper.

Authors' Contributions

Acknowledgments

Supplementary Materials

Supporting information includes NMR spectra for TMA-70, cross-linking, and degradation mechanism of the membranes. Also, thermal, mechanical properties, morphology, hydration results of the membranes, and LSV curves under various conditions are provided. *(Supplementary Materials)*

References

[1] S. Kim, J. H. Han, J. Yuk et al., "Highly selective porous separator with thin skin layer for alkaline water electrolysis," *Journal of Power Sources*, vol. 524, article 231059, 2022.

[2] H. J. Park, S. Y. Lee, T. K. Lee, H.-J. Kim, and Y. M. Lee, "N3-butyl imidazolium-based anion exchange membranes blended with poly(vinyl alcohol) for alkaline water electrolysis," *Journal of Membrane Science*, vol. 611, article 118355, 2020.

[3] N. U. Hassan, E. Motyka, J. Kweder et al., "Effect of porous transport layer properties on the anode electrode in anion exchange membrane electrolyzers," *Journal of Power Sources*, vol. 555, article 232371, 2023.

[4] S. Stiber, N. Sata, T. Morawietz et al., "A high-performance, durable and low-cost proton exchange membrane electrolyser with stainless steel components," *Energy & Environmental Science*, vol. 15, no. 1, pp. 109–122, 2022.

[5] C. Wei, W. Yu, Y. Zhang et al., "Alkaline anion exchange membrane containing pyrene-based π-π stacking interactions," *Journal of Power Sources*, vol. 553, article 232247, 2023.

[6] L. Liu, L. Bai, Z. Liu et al., "Side-chain structural engineering on poly(terphenyl piperidinium) anion exchange membrane for water electrolysers," *Journal of Membrane Science*, vol. 665, article 121135, 2023.

[7] E. J. Park, S. Maurya, M. R. Hibbs, C. H. Fujimoto, K.-D. Kreuer, and Y. S. Kim, "Alkaline stability of quaternized diels–alder polyphenylenes," *Macromolecules*, vol. 52, pp. 5419–5428, 2019.

[8] S. Noh, J. Y. Jeon, S. Adhikari, Y. S. Kim, and C. Bae, "Molecular engineering of hydroxide conducting polymers for anion exchange membranes in electrochemical energy conversion technology," *Accounts of Chemical Research*, vol. 52, no. 9, pp. 2745–2755, 2019.

[9] T. Jiang, C. Wang, T. Wang et al., "Imidazolium structural isomer pyrazolium: a better alkali-stable anion conductor for anion exchange membranes," *Journal of Membrane Science*, vol. 660, article 120843, 2022.

[10] Y. He, L. Wu, J. Pan et al., "A mechanically robust anion exchange membrane with high hydroxide conductivity," *Journal of Membrane Science*, vol. 504, pp. 47–54, 2016.

[11] X. Wang and R. G. H. Lammertink, "Dimensionally stable multication-crosslinked poly(arylene piperidinium) membranes for water electrolysis," *Journal of Materials Chemistry A*, vol. 10, no. 15, pp. 8401–8412, 2022.

[12] J. Ran, L. Wu, B. Wei, Y. Chen, and T. Xu, "Simultaneous enhancements of conductivity and stability for anion exchange membranes (AEMs) through precise structure design," *Scientific Reports*, vol. 4, no. 1, p. 6486, 2014.

[13] N. Chen, C. Hu, H. H. Wang et al., "Poly(alkyl-terphenyl piperidinium) ionomers and membranes with an outstanding alkaline-membrane fuel-cell performance of 2.58 W cm-2," *Angewandte Chemie (International Ed. in English)*, vol. 60, no. 14, pp. 7710–7718, 2021.

[14] X. Su, L. Gao, L. Hu et al., "Novel piperidinium functionalized anionic membrane for alkaline polymer electrolysis with excellent electrochemical properties," *Journal of Membrane Science*, vol. 581, pp. 283–292, 2019.

[15] J. S. Olsson, T. H. Pham, and P. Jannasch, "Functionalizing polystyrene with N-alicyclic piperidine-based cations via Friedel-crafts alkylation for highly alkali-stable anion-exchange membranes," *Macromolecules*, vol. 53, no. 12, pp. 4722–4732, 2020.

[16] J. Dong, H. Li, X. Ren, X. Che, J. Yang, and D. Aili, "Anion exchange membranes of bis-imidazolium cation crosslinked poly(2,6-dimethyl-1,4-phenylene oxide) with enhanced alkaline stability," *International Journal of Hydrogen Energy*, vol. 44, no. 39, pp. 22137–22145, 2019.

[17] X. Chu, Y. Shi, L. Liu, Y. Huang, and N. Li, "Piperidinium-functionalized anion exchange membranes and their application in alkaline fuel cells and water electrolysis," *Journal of Materials Chemistry A*, vol. 7, no. 13, pp. 7717–7727, 2019.

[18] A. M. A. Mahmoud, K. Yoshimura, and Y. Maekawa, "Alkaline fuel cells consisting of imidazolium-based graft-type anion exchange membranes: optimization of fuel cell conditions to achieve high performance and durability," *Journal of Membrane Science*, vol. 620, article 118844, 2021.

[19] W. Li, J. Fang, M. Lv et al., "Novel anion exchange membranes based on polymerizable imidazolium salt for alkaline fuel cell applications," *Journal of Materials Chemistry*, vol. 21, no. 30, p. 11340, 2011.

[20] M. G. Marino and K. D. Kreuer, "Alkaline stability of quaternary ammonium cations for alkaline fuel cell membranes and ionic liquids," *ChemSusChem*, vol. 8, no. 3, pp. 513–523, 2015.

[21] J. Huang, Z. Yu, J. Tang et al., "A review on anion exchange membranes for fuel cells: anion-exchange polyelectrolytes and synthesis strategies," *International Journal of Hydrogen Energy*, vol. 47, no. 65, pp. 27800–27820, 2022.

[22] X. Wang, C. Lin, Y. Gao, and R. G. H. Lammertink, "Anion exchange membranes with twisted poly(terphenylene) backbone: effect of the N-cyclic cations," *Journal of Membrane Science*, vol. 635, article 119525, 2021.

[23] S. Sung, T. S. Mayadevi, K. Min, J. Lee, J. E. Chae, and T.-H. Kim, "Crosslinked PPO-based anion exchange membranes: the effect of crystallinity versus hydrophilicity by oxygen-containing crosslinker chain length," *Journal of Membrane Science*, vol. 619, article 118774, 2021.

[24] B. Lin, F. Xu, F. Chu, Y. Ren, J. Ding, and F. Yan, "Bis-imidazolium based poly(phenylene oxide) anion exchange membranes for fuel cells: the effect of cross-linking," *Journal of Materials Chemistry A*, vol. 7, no. 21, pp. 13275–13283, 2019.

[25] R. A. Becerra-Arciniegas, R. Narducci, G. Ercolani et al., "Alkaline stability of model anion exchange membranes based on poly(phenylene oxide) (PPO) with grafted quaternary ammonium groups: influence of the functionalization route," *Polymer*, vol. 185, article 121931, 2019.

[26] Y. Yang, P. Li, X. Zheng et al., "Anion-exchange membrane water electrolyzers and fuel cells," *Chemical Society Reviews*, vol. 51, no. 23, pp. 9620–9693, 2022.

[27] X. Du, H. Zhang, Y. Yuan, and Z. Wang, "Constructing microphase separation structure to improve the performance of anion-exchange membrane based on poly(aryl piperidinium) cross-linked membranes," *Journal of Power Sources*, vol. 487, article 229429, 2021.

[28] K. Yang, X. Chu, X. Zhang et al., "The effect of polymer backbones and cation functional groups on properties of anion exchange membranes for fuel cells," *Journal of Membrane Science*, vol. 603, article 118025, 2020.

[29] K. Min, Y. Lee, Y. Choi, O. J. Kwon, and T.-H. Kim, "High-performance anion exchange membranes achieved by cross-linking two aryl ether-free polymers: poly(bibenzyl N-methyl piperidine) and SEBS," *Journal of Membrane Science*, vol. 664, article 121071, 2022.

[30] L. Li, J. Zhang, T. Jiang et al., "High ion conductivity and diffusivity in the anion exchange membrane enabled by tethering with multication strings on the poly(biphenyl alkylene) backbone," *ACS Applied Energy Materials*, vol. 3, no. 7, pp. 6268–6279, 2020.

[31] N. Chen, S. Y. Paek, J. Y. Lee, J. H. Park, S. Y. Lee, and Y. M. Lee, "High-performance anion exchange membrane water electrolyzers with a current density of 7.68 A cm^{-2} and a durability of 1000 hours," *Energy & Environmental Science*, vol. 14, no. 12, pp. 6338–6348, 2021.

[32] Q. Chen, Y. Huang, X. Hu et al., "A novel ion-solvating polymer electrolyte based on imidazole-containing polymers for alkaline water electrolysis," *Journal of Membrane Science*, vol. 668, article 121186, 2023.

[33] W. Yang, P. Xu, X. Li et al., "Mechanically robust semi-interpenetrating polymer network via thiol-ene chemistry with enhanced conductivity for anion exchange membranes," *International Journal of Hydrogen Energy*, vol. 46, no. 17, pp. 10377–10388, 2021.

[34] C. Liu, F. Cheng, B. Liu et al., "Versatile, oxygen-insensitive surface-initiated anionic polymerization to prepare functional polymer brushes in aqueous solutions," *Langmuir*, vol. 38, no. 3, pp. 1001–1010, 2022.

[35] M. Mandal, G. Huang, N. U. Hassan, W. E. Mustain, and P. A. Kohl, "Poly(norbornene) anion conductive membranes: homopolymer, block copolymer and random copolymer properties and performance," *Journal of Materials Chemistry A*, vol. 8, no. 34, pp. 17568–17578, 2020.

[36] Z. Li, R. Yu, C. Liu et al., "Preparation and characterization of side-chain poly(aryl ether ketone) anion exchange membranes by superacid-catalyzed reaction," *Polymer*, vol. 222, article 123639, 2021.

[37] X. Li, K. Yang, Z. Wang et al., "Chain architecture dependence of morphology and water transport in poly(fluorene alkylene)-based anion-exchange membranes," *Macromolecules*, vol. 55, no. 23, pp. 10607–10617, 2022.

[38] S. Zhang, Y. Wang, P. Liu, X. Wang, and X. Zhu, "Photo-cross-linked poly(N-allylisatin biphenyl)-co-poly(alkylene biphenyl)s with pendant N-cyclic quaternary ammonium as anion exchange membranes for direct borohydride/hydrogen peroxide fuel cells," *Reactive and Functional Polymers*, vol. 152, article 104576, 2020.

[39] T. H. Pham, J. S. Olsson, and P. Jannasch, "Poly(arylene alkylene)s with pendant N-spirocyclic quaternary ammonium cations for anion exchange membranes," *Journal of Materials Chemistry A*, vol. 6, no. 34, pp. 16537–16547, 2018.

[40] I. Matanovic, S. Maurya, E. J. Park, J. Y. Jeon, C. Bae, and Y. S. Kim, "Adsorption of polyaromatic backbone impacts the performance of anion exchange membrane fuel cells," *Chemistry of Materials*, vol. 31, no. 11, pp. 4195–4204, 2019.

[41] D. Li, E. J. Park, W. Zhu et al., "Highly quaternized polystyrene ionomers for high performance anion exchange membrane water electrolysers," *Nature Energy*, vol. 5, no. 5, pp. 378–385, 2020.

[42] K. Zhang, M. B. McDonald, I. E. A. Genina, and P. T. Hammond, "A highly conductive and mechanically robust OH–conducting membrane for alkaline water electrolysis," *Chemistry of Materials*, vol. 30, no. 18, pp. 6420–6430, 2018.

[43] L. A. Diaz, R. E. Coppola, G. C. Abuin, R. Escudero-Cid, D. Herranz, and P. Ocón, "Alkali-doped polyvinyl alcohol-polybenzimidazole membranes for alkaline water electrolysis," *Journal of Membrane Science*, vol. 535, pp. 45–55, 2017.

[44] C.-H. Huang, H.-M. Wu, C.-C. Chen, C.-W. Wang, and P.-L. Kuo, "Preparation, characterization and methanol permeability of proton conducting membranes based on sulfonated ethylene-vinyl alcohol copolymer," *Journal of Membrane Science*, vol. 353, no. 1-2, pp. 1–9, 2010.

[45] J. M. Lagaron, A. K. Powell, and G. Bonner, "Permeation of water, methanol, fuel and alcohol-containing fuels in high-barrier ethylene-vinyl alcohol copolymer," *Polymer Testing*, vol. 20, no. 5, pp. 569–577, 2001.

[46] H. S. Mansur, C. M. Sadahira, A. N. Souza, and A. A. P. Mansur, "FTIR spectroscopy characterization of poly (vinyl alcohol) hydrogel with different hydrolysis degree and chemically crosslinked with glutaraldehyde," *Materials Science and Engineering*, vol. 28, no. 4, pp. 539–548, 2008.

[47] X. Wang, "Poly (vinyl alcohol)/graphene nanocomposite hydrogel scaffolds for control of cell adhesion," *Journal of Renewable Materials*, vol. 8, no. 1, pp. 89–99, 2020.

[48] N. Li, L. Wang, and M. Hickner, "Cross-linked comb-shaped anion exchange membranes with high base stability," *Chemical Communications*, vol. 50, no. 31, pp. 4092–4095, 2014.

[49] Y. Li, Y. Liu, A. M. Savage et al., "Polyethylene-based block copolymers for anion exchange membranes," *Macromolecules*, vol. 48, no. 18, pp. 6523–6533, 2015.

[50] K. H. Lim, A. S. Lee, V. Atanasov et al., "Protonated phosphonic acid electrodes for high power heavy-duty vehicle fuel cells," *Nature Energy*, vol. 7, no. 3, pp. 248–259, 2022.

[51] J. Jung, K. H. Lim, S. Maurya et al., "Dispersing agents impact performance of protonated phosphonic acid high-temperature polymer electrolyte membrane fuel cells," *ACS Energy Letters*, vol. 7, no. 5, pp. 1642–1647, 2022.

[52] P. Knauth, L. Pasquini, R. Narducci, E. Sgreccia, R. A. Becerra-Arciniegas, and M. L. Di Vona, "Effective ion mobility in anion exchange ionomers: relations with hydration, porosity, tortuosity, and percolation," *Journal of Membrane Science*, vol. 617, article 118622, 2021.

[53] H.-S. Dang and P. Jannasch, "A comparative study of anion-exchange membranes tethered with different hetero-cycloaliphatic quaternary ammonium hydroxides," *Journal of Materials Chemistry A*, vol. 5, no. 41, pp. 21965–21978, 2017.

[54] L. Pasquini, M. L. Di Vona, and P. Knauth, "Effects of anion substitution on hydration, ionic conductivity and mechanical properties of anion-exchange membranes," *New Journal of Chemistry*, vol. 40, no. 4, pp. 3671–3676, 2016.

[55] F. Razmjooei, A. Farooqui, R. Reissner, A. S. Gago, S. A. Ansar, and K. A. Friedrich, "Elucidating the performance limitations of alkaline electrolyte membrane electrolysis: dominance of anion concentration in membrane electrode assembly," *ChemElectroChem*, vol. 7, no. 19, pp. 3951–3960, 2020.

[56] A. Guha, M. Sahoo, K. Alam, D. K. Rao, P. Sen, and T. N. Narayanan, "Role of water structure in alkaline water electrolysis," *iScience*, vol. 25, no. 8, 2022.

[57] G. C. Anderson, B. S. Pivovar, and S. M. Alia, "Establishing performance baselines for the oxygen evolution reaction in alkaline electrolytes," *Journal of the Electrochemical Society*, vol. 167, no. 4, article 044503, 2020.

[58] M. S. Cha, J. E. Park, S. Kim et al., "Poly (carbazole)-based anion-conducting materials with high performance and durability for energy conversion devices," *Energy & Environmental Science*, vol. 13, no. 10, pp. 3633–3645, 2020.